

## Research Article

# Spatial variability of sedimentological properties in a large Siberian lake

Thomas Kumke<sup>1,\*</sup>, Annemarieke Schoonderwaldt<sup>2</sup> and Ulrike Kienel<sup>3</sup>

<sup>1</sup> Alfred-Wegener-Institute for Polar and Marine Research, Research Department Potsdam, Telegrafenberg A43, 14473 Potsdam, Germany

<sup>2</sup> University of Leipzig, Department of Geology, Talstrasse 35, 04103 Leipzig, Germany

<sup>3</sup> GeoForschungsZentrum Potsdam, Telegrafenberg C327, 14473 Potsdam, Germany

Received: 15 January 2004; revised manuscript accepted: 19 August 2004

**Abstract.** The analysis of spatial variability of lake sediment properties in Lake Lama, Central Siberia is presented. The aims were to characterize the spatial structure in lake sediment composition, to determine major spatial patterns of sediment properties by calculating estimates at locations where no samples were available, and to assess the main processes determining these patterns. Sediment properties were measured at 71 spatially distributed locations in the lake, comprising particle size distribution, biogeochemical properties such as total organic carbon, total nitrogen or stable carbon isotopes, as well as geochemical distribution of major and trace elements. Spatial analysis consisted of a principal components analysis and, subsequently, calculation and modelling of variograms to describe the spatial structure in the data as well as determination of spatial estimates using block-kriging to map spatial structure. The results showed that particle

size, biogenic silica, CaO,  $\delta^{13}\text{C}_{\text{org}}$ , Zr and TOC/TN ratio were a major source of variability in sediment properties and, thus, dominate the sediment structure in Lake Lama. Major anomalies occurred near river inlets, depending on river size and its position as well as slope of the river bed. Other anomalies were associated with water depths, morphology of the lake basins, and wind-induced currents and re-suspension in the shallow part of the western basin. The spatial structure in sediment properties indicate that several processes act at different spatial scales. Moreover, there was a considerable amount of small-scale variability that could not be quantified due to sampling design. The results showed that heterogeneity in lake sediment composition is a main characteristic of large lake systems, and must be taken into account, especially in paleolimnological and environmental applications.

**Key words.** Geochemistry; heterogeneity; lake sediments; Siberia; spatial structure; variogram.

## Introduction

Spatial heterogeneity in sedimentological, geochemical and biogeochemical properties is one main characteristic of lake sediments. The spatial distribution in these properties depends on processes such as current, turbulence, chemical precipitation and turbidity, on physical factors

like lake morphology, and on catchment characteristics like underlying geology, the number and size of inflows, meltwater input and land use (Håkanson and Jansson, 1983; Ashley, 1995). In general, the spatial variability in sediment composition is thought to increase with lake size and the number and size of the inflows, or in other words, with the increasing number of processes affecting the lake (Pinel-Alloul, 1995; Kienel and Kumke, 2002). Most often, the variability in lake systems is structured, meaning that spatially distributed data are autocorrelated (i.e., a spatially ordered variable is correlated with itself).

\* Corresponding author phone: 00493312882165;  
e-mail: tkumke@awi-potsdam.de  
Published on Web: March 2, 2005

Spatial autocorrelation is often strong for data points closely spaced and weak or even non-significant for data points far apart. For example, Kienel and Kumke (2002) showed that the distribution in fossil diatom composition is spatially autocorrelated up to 55 km in Lake Lama, Central Siberia, depending on water depth and river input. Lebo and Reuter (1995) suggested a dependency of organic C, N, P and particle size fractions on water depth of a large lake using data from 32 surficial sediment samples. While the studies of Lebo and Reuter (1995) and Kienel and Kumke (2002) were carried out on large, deep lakes, the work of Anderson (1990; 1998) implies that the spatial variability in sedimentary diatom composition and accumulation rate also occurs in small lakes with simple morphology. Korsman et al. (1999) discussed the variability in surface sediment composition of a small Swedish lake shown by near-infrared spectroscopy (NIR) and loss-on-ignition (LOI), revealing spatial patterns influenced by wastewater input, clear-cut forest and transport of allochthonous material.

The methodology of analyzing spatial variation in sediment properties in each study differed. For example, Korsman et al. (1999) used principal component scores of NIR spectra to draw contour maps for interpretation. Kienel and Kumke (2002) used a more sophisticated analysis of spatial variability in lake sediments, based on geostatistical analysis of sample scores from correspondence analysis (CA). Geostatistics is an effective method to analyze spatial variation and has been widely used in geology, hydrology, soil science and ecology (Russo, 1984; Webster, 1985; Legendre and Fortin, 1989; Ellsworth and Boast, 1996; Kumke et al., 1999; 2002). The aim of geostatistical analysis is twofold: (i) calculation and modeling of spatial structure in data by means of variograms, and (ii) calculation of estimates at locations where no data are available using the kriging technique, an optimal-weighted interpolation technique (for a review of geostatistical methods see Isaaks and Srivastava, 1989; Webster and Oliver, 2000). The main advantage of geostatistical analysis is that scale and direction of autocorrelation in data are accounted for.

Analysis of sedimentological measurements is complex because data consist of a multivariate ensemble of variables that are often interrelated. Ordination techniques provide an effective tool to reduce the dimensionality in such data (Legendre and Legendre, 1998). If data are quantitative and their relationships are presumed to be linear, principal components analysis (PCA) is an appropriate ordination technique (Ter Braak and Prentice, 1988). Principal components analysis is an eigenvector technique that reduces the multidimensional data set to a few principal axes, thereby decomposing the total variance in the data. The first few axes represent most of the variance in the data. In PCA, eigenvectors and principal component scores are calculated and the latter can

be used for further spatial analysis as carried out, for example, in Korsman et al. (1999) and Kienel and Kumke (2002).

Generally, the sediment composition of lakes provides useful information about regional changes in environmental history, such as land use changes in the catchment, eutrophication or pollution history. Examination of spatial variation allows one to assess the different processes affecting sediment variability and their impact on the lake and its habitats. In terms of paleolimnological considerations, quantifying the spatial variability in surface sediment composition is important to estimate the representativity of paleolimnological studies.

Here, the surface sediment composition of a large lake in Central Siberia was studied using measurements of biogeochemistry, particle size distribution and geochemical element distribution at 71 locations spatially distributed in the lake. The aim of this paper is threefold: (i) to determine and characterize the spatial structure in lake sediment composition, (ii) to estimate the sediment composition at locations where no measurements were available, thereby obtaining major spatial patterns in sediment properties, and (iii) to assess primary physical and hydrological processes that determine spatial patterns. A sound knowledge about these processes is required for further studies on the lake to solve paleolimnological, paleoclimatological and ecological problems. Lake Lama is an excellent example on the complexity of features in large lakes and their influence on lake sediment characteristics. This paper shows how to analyze such features using geostatistical techniques new to the field of lake sedimentology.

### Study area

Lake Lama (69°33'N, 90°13'E) is located in the northwest foothills of the Putoran Plateau near the city of Norilsk, Central Siberia. The lake is of tectonic origin, about 80 km × 13 km in size and up to 254 m deep. It consists of an eastern (II) and a western basin (IV) connected by a north-south trending subbasin (III), and an eastern tip (I; Fig. 1). It is surrounded by steeply-sloped mountains to the north and south that reach altitudes of 1234 m a.s.l.

The largest part of the catchment is on Late Permian to Late Triassic Continental Flood Basalts (CFBs) and associated tuffs of the Siberian Trap. The CFBs have been subdivided into 11 lava types, suites or formations (Lightfoot et al., 1990). The subdivisions were based on differences in geochemical characteristics among the suites, in CaO and MgO content. The geochemistry is generally independent of textural properties. A range of mafic to ultra-mafic intrusions have been formed in the region, and are generally rich in nickel, copper, sulfide and platinum. The geology of the western part of the catch-

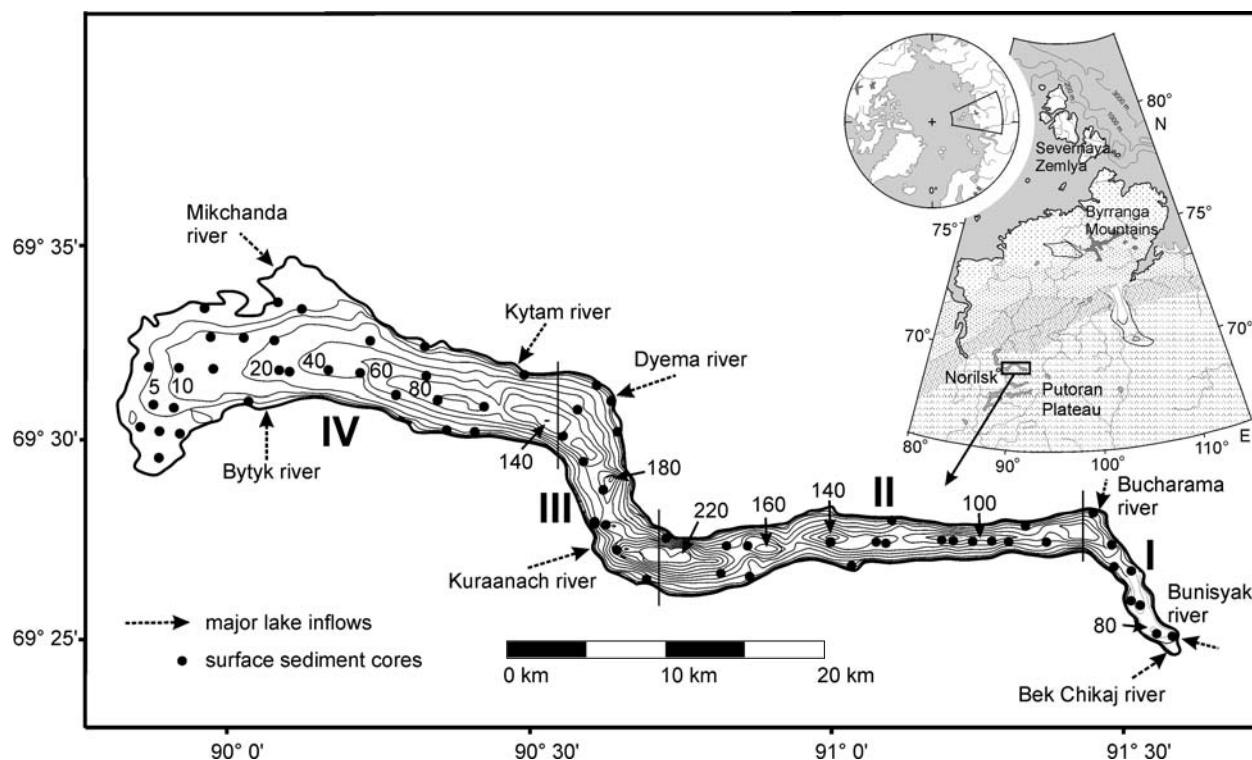


**Figure 1.** Map of Lake Lama and the coring locations. The values given on the isolines are water depths [m]. Roman numerals denote subregions of the lake as used in the text: I – eastern tip; II – eastern basin; III – north-south trending subbasin; IV – western basin. The vertical lines indicate the borders between the subregions.

ment is dominated by Quaternary lacustrine, glacial, glacial and alluvial deposits. In the western catchment occurs some outcrops of Lower Palaeozoic to Late Permian sedimentary rocks formed in a structural depression called the Tunguska Syncline. The sequence contains marine dolomites, limestones and agillites, calcareous and dolomitic marls, sulfate-rich evaporites, shallow water limestones, and lagoonal and continental sediments (e.g., siltstone and sandstone; Lightfoot et al., 1990). Structurally, the area is characterized by several pre- and post-trap positive and negative structures (uplift forms and basins) and fault systems of different orientation (Naldrett et al., 1992).

The regional climate around Lake Lama is continental. Annual temperatures fluctuate considerably. Average annual air temperature is  $-9.8^{\circ}\text{C}$  with mean January air temperatures between  $-25$  and  $-35^{\circ}\text{C}$  and mean July air temperatures ranging from  $10$  to  $15^{\circ}\text{C}$ . Annual precipitation is high compared to other areas in Central Siberia (Harwart, 1999). The main wind direction is east to north-east (Hagedorn et al., 1999). Lake Lama is ice-covered from October to May. Thawing starts in May and takes about one month. Lake Lama can be classified as a sub-polar dimictic to polar monomictic lake type based on water column temperature profiles (Kienel and Kumke, 2002). The catchment is about  $6210\text{ km}^2$ . More than 10 large inflows enter Lake Lama, the largest being the

Mikchanda River with a delta on its north-west shore (Fig. 1). The lake drains west via Lake Melkoye into Lake Pyasino. The inundated shore line reaches up to 10 m in width and is covered with pebbles, gravel and sand. At high lake levels, vegetation near the shoreline is submerged. Sparsely distributed macrophytes (*Chara* sp.) were observed in well-illuminated places.

Vegetation of the study area is forest tundra, and is dense and dominated by Taiga trees and shrubs. The taiga forest consists of spruce (*Picea obovata*), larch (*Larix czekanovskii* and *L. sibirica*) and birch (*Betula pubescens*). The upper forest boundary is located between 200–400 m a.s.l. (Galaziy and Parmuzin, 1981), where larch and shrubs form an open forest (Andreev et al., 2004). Shrubs include dwarf birch (*Betula nana*), shrub alder (*Alnus fruticosa*), juniper (*Juniperus communis*) and willow (*Salix* spp.).

## Methods

### Sediment sampling and measurements

A total of 71 surface sediment samples (Fig. 1) were collected during summer 1997. Sediment coring took place from a swimming platform using a light gravity corer (Kajak et al., 1965) that allowed undisturbed recovery of soft upper sediments. The core samples contain 2 cm

of surface sediments. Sampling positions were estimated using a Geographic Positioning System (Trimble Scout/Scoutmaster GPS™ accurate to ±100 m).

All analytical procedures were carried out on freeze-dried samples. Samples were oxidized and disaggregated by means of 3–10% H<sub>2</sub>O<sub>2</sub> solution for estimating the particle size distribution. The sand fraction was separated by wet sieving (63 μm mesh). Clay and silt fractions were separated by an Atterberg cylinder, which uses differences in settling velocity between the fractions.

Total carbon (TC), total organic carbon (TOC), total nitrogen (TN) and total sulphur (TS) fractions as well as stable isotope composition of organic carbon ( $\delta^{13}\text{C}_{\text{org}}$ ) were analyzed. The TC, TN and TS fractions were measured on homogenized subsamples (10 mg) by a CNS-932 micro-analyzer (LECO) that combusts samples at 1100 °C. The TOC fraction was determined by combusting samples at 1400 °C using a Metalyt-CS analyzer (ELTRA). Before measurement, samples were treated with hydrochloric acid to remove carbonates. The carbonate fraction was estimated by multiplying the difference between TC and TOC by a constant  $c = 8.33$ . The  $\delta^{13}\text{C}_{\text{org}}$  contents were measured using an elemental analyzer (HERAEUS) and MAT Delta S mass-spectrometer (FINNIGAN).

Major and trace elements of sediment were measured by X-ray fluorescence spectrometry (SRS 3000, SIEMENS). Measurements were carried out on glass tablets produced in a fused mass method using 0.6 g crushed, pre-dried and glow-d material. Major elements included Si, Ti, Al, Fe, Mn, Mg, Ca, Na, K and P, whereas trace elements included Ce, Co, Cr, Cu, Nb, Ni, Pb, Rb, Sr, V, Y, Zn and Zr. The biogenic silica content was estimated using spectrophotometry. Since all elements were measured as fractions of sediment, they were normalized to the Al fraction to obtain absolute variations (Harwart, 1999).

### Statistical methods

Prior to ordination, all variables were examined for extreme values and statistical distributions. Extreme values were removed when they deviated by more than four standard deviations (SD) from the mean. Since variables are assumed to be normally distributed in ordination techniques, variables with skewed distributions were transformed using an appropriate transformation (Webster and Oliver, 2000). Principal components analysis (PCA) was performed to reduce the dimensionality and to simplify the variation structure in the data. For PCA, the matrix  $\mathbf{Y}$  of the measured variables was converted into a correlation matrix  $\mathbf{R}$  because of the different dimensions of the data (Legendre and Legendre, 1998). The principle axes of variation were found by solving the characteristic equation for  $\mathbf{R}$  and calculating the eigenvalue  $\lambda$  for each

principle axis  $k$  as well as the eigenvector  $\mathbf{u}_k$  associated to  $\lambda_k$ . The position of sites (i.e., the principal component scores) are a linear combination of the standardized values for each variable and the eigenvectors, that is:

$$\mathbf{F} = \left( \frac{y_{ij} - \bar{y}_j}{SD_j} \right) \mathbf{U} \quad (1)$$

where  $y_j$  is the measured value for each variable  $j$ ,  $SD_j$  is the standard deviation and  $\mathbf{U}$  is the matrix of eigenvectors. The principal component scores  $\mathbf{F}$  are weighted averages of all variables in the system. Principal component scores of the first axis are most representative of the data by accounting for most of the variance. The results of PCA were analyzed using a graphical biplot of  $\mathbf{U}$  and  $\mathbf{F}$  of two principle axes.

Analysis of spatial variability was carried out by variogram modeling of the principal component scores  $f_{ik}$  for axis  $k$  derived from PCA. The omnidirectional semi-variances were estimated using:

$$\gamma(\mathbf{h}) = \frac{1}{2N(\mathbf{h})} \sum_{i=1}^{N(\mathbf{h})} \{z(\mathbf{x}_i) - z(\mathbf{x}_i + \mathbf{h})\}^2 \quad (2)$$

where  $\gamma$  is the semi-variance,  $\mathbf{h}$  is the lag distance (m),  $N(\mathbf{h})$  is the number of pairs at each lag distance, and  $z$  is the value at the sampling point  $x_i$  (i.e., the principal component scores  $f_{ik}$  for axis  $k$ ). The lag distance is the separation distance between two sampling points from which the squared differences were calculated. The experimental variogram was plotted using the calculated semi-variances  $\gamma$  versus each lag distance  $h$  (Webster and Oliver, 2000). Theoretical variogram functions were fitted to experimental variograms using a least-squares approach. Variogram models were examined using cross-validation techniques (Russo, 1984). Cross-validation was performed by excluding a sampling point, estimating a value for this point, and calculating the residual. The mean square of residuals is the mean squared prediction error (MSPE) and serves as a measure of accuracy for the variogram model (Kumke, 1999).

Subsequent mapping of principal component scores of axis  $k$  was achieved by obtaining estimates of principal component scores using block kriging. Kriging is an unbiased interpolation method in which estimates of a variable  $z^*$  at unknown positions are weighted linear combinations of  $z(x_k)$ :

$$z^*(x_0) = \sum_{i=1}^n w_i z(x_i) \quad (3)$$

where  $w_i$  denotes the weight given to each principal component score. To derive unbiased estimates, the weights sum to unity. Weights depend on the shape and magnitude of the variogram model (Isaaks and Srivastava, 1989). For block kriging, the spatial field was decomposed into

blocks of 700 m × 350 m to derive average block estimates of  $z$  ( $x_k$ ).

All numerical analyses were carried out using CANOCO 4.0 (Ter Braak and Smilauer, 1998) for ordination, and GEOPACK 1.0 (Yates and Yates, 1990) and GEOEAS 1.2.1 (Englund and Sparks, 1991) for variogram analysis and kriging, respectively.

## Results and discussion

### Summary of the sedimentological measurements

Summary statistics of surface sediment properties of Lake Lama are given in Table 1. According to the average par-

ticle size distribution, the sediment can be characterized as a silty loam. However, coefficients of variation (CVs) are, especially for the sand fraction, quite large and show a remarkable local variability. A high local variability of the sand fraction is indicated by the large ratio between the mean and median, which is typical if there are some extremely large values outside the population distribution. These large values of the sand fraction were observed near river mouths in the steep sides along the eastern part of the lake and caused by deposition of inserted coarse material.

In general, biogenic components were characterized by relatively low fractions of TC, TN and TS. Their CVs were quite similar (ca. 40 to 50%) and common for

**Table 1.** Summary statistics for (a) biogeochemical and sedimentological, and (b) geochemical measurements. All percentages are related to dry mass.

Variable	Unit	(a)				
		Mean	Median	SD	CV	Skewness
Si <sub>am</sub>	%	6.01	6.07	2.62	43.54	0.26
TC	%	1.13	1.05	0.59	51.95	2.52
TN	%	0.10	0.10	0.04	37.51	-0.31
TOC	%	1.14	1.08	0.59	51.79	2.29
CaCO <sub>3</sub>	%	0.17	0.00	0.32	190.81	2.21
TS	%	0.01	0.01	0.01	52.22	1.65
δ <sup>13</sup> C <sub>org</sub>	‰ V-PDB	-26.31	-26.67	1.24	4.70	1.93
TOC/TN		12.20	10.83	3.84	31.46	1.73
Sand	%	17.23	2.35	24.69	143.25	1.28
Silt	%	54.88	59.65	18.84	34.33	-0.92
Clay	%	27.60	26.98	12.06	43.69	-0.08
Variable	Unit	(b)				
		Mean	Median	SD	CV	Skewness
SiO <sub>2</sub>	%	22.74	22.75	0.67	2.95	-0.27
TiO <sub>2</sub>	%	0.69	0.69	0.05	7.92	0.54
Al <sub>2</sub> O <sub>3</sub>	%	4.01	4.05	0.19	4.71	-0.81
Fe <sub>2</sub> O <sub>3</sub>	%	3.49	3.46	0.20	5.77	0.21
MnO	%	0.16	0.15	0.04	22.12	3.53
MgO	%	3.63	3.62	0.32	8.74	0.43
CaO	%	6.31	6.26	0.81	12.91	0.16
Na <sub>2</sub> O	%	0.67	0.67	0.06	9.35	1.33
K <sub>2</sub> O	%	0.29	0.29	0.06	19.04	0.82
P <sub>2</sub> O <sub>5</sub>	%	0.03	0.03	0.01	21.70	0.56
Loi	%	5.41	5.50	1.18	21.78	-0.32
Ba	ppm	253.76	247.00	40.34	15.90	0.71
Ce	ppm	72.75	72.00	14.28	19.63	0.39
Co	ppm	49.37	49.00	4.46	9.04	0.13
Cr	ppm	160.33	154.00	22.70	14.16	0.96
Cu	ppm	95.91	96.00	33.86	35.30	-0.61
Nb	ppm	12.43	12.00	1.97	15.88	0.61
Ni	ppm	88.12	89.00	9.84	11.17	-0.79
Pb	ppm	30.88	22.50	19.16	62.07	1.40
Rb	ppm	22.72	22.00	5.29	23.27	0.55
Sr	ppm	226.31	227.00	19.26	8.51	-0.14
V	ppm	242.94	234.00	30.79	12.67	0.62
Y	ppm	15.49	15.00	2.20	14.23	0.47
Zn	ppm	94.57	93.00	12.89	13.63	1.36
Zr	ppm	98.51	98.00	11.18	11.35	0.24

field-measured quantities (Kumke et al., 1999; 2002). The mean to median ratio were approximately 1.0, indicating no extreme values. The TOC/TN ratio had mean and median values that were in the range typical of autochthonous-derived organic matter (Meyers and Ishiwatari, 1995). However, there were some localities with values  $>20$  that might be caused by the introduction of allochthonous material (Meyers and Ishiwatari, 1995). The geochemical element distribution had, in general, relatively low CVs with a few exceptions. The ratio between the mean and median is near unity for most elements except for Cu and Pb. Both, Cu and Pb had extreme values at some localities in the eastern basin, thus explaining their relatively large CVs.

### Biplot analysis

The PCA of all sedimentological measurements resulted in a distance biplot of the first two principal axes shown in Fig. 2. The first and second axis explained 34% and 18% of the variance, respectively. Sites were classified according to their spatial position in the basins of the lake. There were no structuring of sites along the first axis in respect to that classification. However, an interesting feature was that most sampling sites from the western

basin were located in the second and third quadrant of the plot, indicating the western basin has sediments high in silt and clay as well as being rich in some biogeochemical components such as biogenic silica ( $Si_{am}$ ) and TN. Variables that contribute most to the first axis were particle size fractions,  $Si_{am}$ , TN, the ratio of TOC/TN, and the major elements  $Na_2O$ ,  $TiO_2$ ,  $CaO$ ,  $MgO$ ,  $Fe_2O_3$  and  $P_2O_5$ . Principal component scores were well-structured according to the classification criterion along the second axis. Almost every sample from the western basin had a positive principal component score for PC2, whereas samples of the other three basins were located in the third and fourth quadrant of the plot. Thus, basin morphology and water depths determined a large extent of the second axis. Additionally, there was a significant negative correlation between principal component scores of the second axis and water depth ( $r = -0.36$ ,  $P \leq 0.05$ ) supporting this observation. The most important variables, which covary with the second axis, were  $\delta^{13}C_{org}$ ,  $K_2O$ ,  $SiO_2$ , the ratio of TOC/TN, and the trace elements Ba, Zr, Nb, Ce and Cu. Some of these (such as  $\delta^{13}C_{org}$  and Ba) are partially correlated to water depth.

The third and the fourth principal axes represented 9.6% and 6.2% of the explained variance, respectively. However, biplot analyses using the third and fourth axes (not shown) yielded no structure.

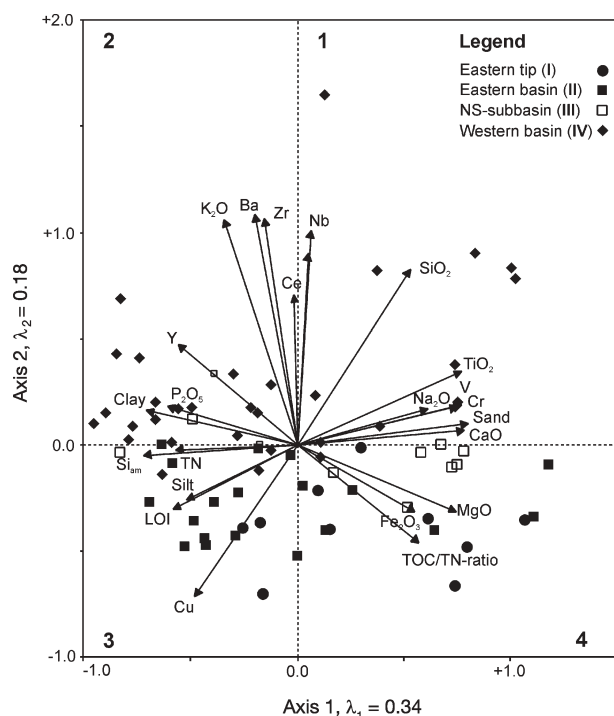


**Figure 2.** Distance biplot of PCA conducted on sediment properties of Lake Lama. The first and second PCs are plotted alongside with the contribution of each variable. All variables are shown that fit into the variable space with  $\geq 10\%$  of the variance explained. Arabian numbers indicate the number of the quadrant used in the text.

### Variogram analysis

Using principal component scores of the first two axes, a variogram analysis was carried out. Both variograms are spatially structured (Fig. 3) and have typical variogram features, i.e., a range (part of the curve where the semi-variances increase with increasing lag distance), a sill (part of the curve where the semi-variance is at its maximum and independent of  $h$ ) and a nugget variance (i.e., semi-variance at  $h = 0$ ). The variogram of the first axis scores has small semi-variances at short lags that rise to values independent of  $h$  at a length of about 5 km. There is a decrease in semi-variances from 30 km to 36 km followed again by an increase. This phenomenon is the so-called 'hole effect' (Webster and Oliver, 2000) and most often has some physical reason. Variogram analysis revealed that sampling points in the eastern tip and eastern basin near river mouths (locations with large positive principal component scores) contributed to the low semi-variances at distances of 30 and 32 km. At lags of about 34 and 36 km, sampling points in the eastern basin (locations with negative principal component scores) separated by these distances contributed largely to the semi-variances. Physical processes leading to the increased similarities in sediment properties at these lags are not clear but they are partly related to riverine input of material. The nugget variance is considerably high, leading to a nugget to sill ratio of 34%. Thus, about one third of the

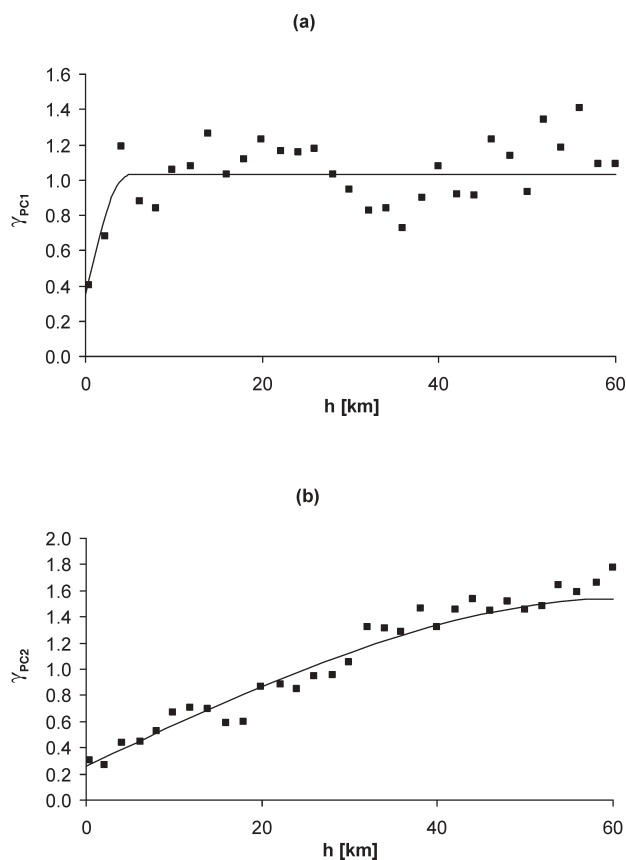


**Figure 3.** Variogram of the PCs of the first two principal axes and their fitted models. A summary of model parameters is given in Table 2.

variation is related to random fluctuations, measurement errors or small-scale processes beyond our scale of measurement (Webster and Oliver, 2000; Kienel and Kumke, 2002). Since there are some biogeochemical variables such as biogenic silica and TN contributing to that variogram, biotic processes like small-scale variations in primary productivity or nutrient uptake by aquatic organisms might be responsible for the nugget variance. The variogram of the second axis has a long range of spatial correlation of approximately 61 km. This long range is probably caused by water depth since there is a significant correlation between water depth and component scores of the second axis. A similar phenomenon was observed by the spatial analysis of diatom assemblages in the same lake (Kienel and Kumke, 2002). However, unlike the spatial structure in diatom assemblages, this variogram has a noticeable relative nugget variance of about 21%.

The number of pairs used for the calculation of variograms range between 50 and 396, sufficiently large to estimate a reliable variogram. Variogram analysis could not be extended into different directions due to the lack of available pairs. We fitted spherical models to both variograms; their model parameters as well as the results of the cross-validation procedure are given in Table 2. The

**Table 2.** Fitted standardized variogram model parameters, mean squared prediction error (MSPE), residual error (RE) and its standard deviation for the object scores of PCA axes 1 and 2.

	PCA axis 1	PCA axis 2
Model	spherical	spherical
Range (km)	4.88	61.0
Sill	1.03	1.79
Nugget	0.35	0.37
MSPE	0.24	0.01
RE	0.01	-0.05

prediction error (MSPE) is low, especially for the model of the second axis. The residual error (RE) is close to zero, indicating no systematic error in the models (Russo, 1984). Variograms of the third and fourth axes also were estimated (not shown), but they showed no spatial structuring. For the variogram of the PCs of axis 3, a nugget model could be fitted that indicates every variability of the site scores is generated by random processes.

#### Spatial distribution of the sediment characteristics in Lake Lama

Block-kriged estimates of principal component scores of the first two axes (Fig. 4) revealed a distinct spatial structuring in sediment properties in Lake Lama. The spatial distribution in the estimation error (not presented) showed no systematic features. Thus, estimates are non-related to their error (Isaaks and Srivastava, 1989; Webster and Oliver, 2000).

The distribution of site score estimates for axis 1 varied at relatively small scales (Fig. 4a). There are some steep spatial gradients in estimates that occur near river inflows in the eastern tip as well as in the north-south connected basin, towards the northern shore of the western basin and in the shallow part near the outflow of the western basin. High positive estimates occurring near river mouths, e.g., the Rivers Bek Chikaj, Kuraanach, Dyema and partly Bucharama, are associated with large fractions of sand and higher values in TOC/TN ratio and CaO content. The large sand fractions at river inlets are most probably caused by the transport and subsequent sedimentation of coarse-grained material in the lake. Sediments at sample locations containing large fractions of sand also have a distinctly higher percentage of diatoms typical of rivers (Kienel and Kumke, 2002). In addition, the sand fraction was positively correlated with CaO ( $r = 0.76$ ,  $P \leq 0.05$ ). Higher values of TOC/TN ratios at river mouths mostly are significantly larger than the whole lake average of about 12.2, indicating that the sediments are affected more by material from land plants than elsewhere in the lake. Apart from these locations, TOC/TN values of sediments in Lake Lama point to a dominance of autochthonous production (Meyers and Ishiwatari, 1995).

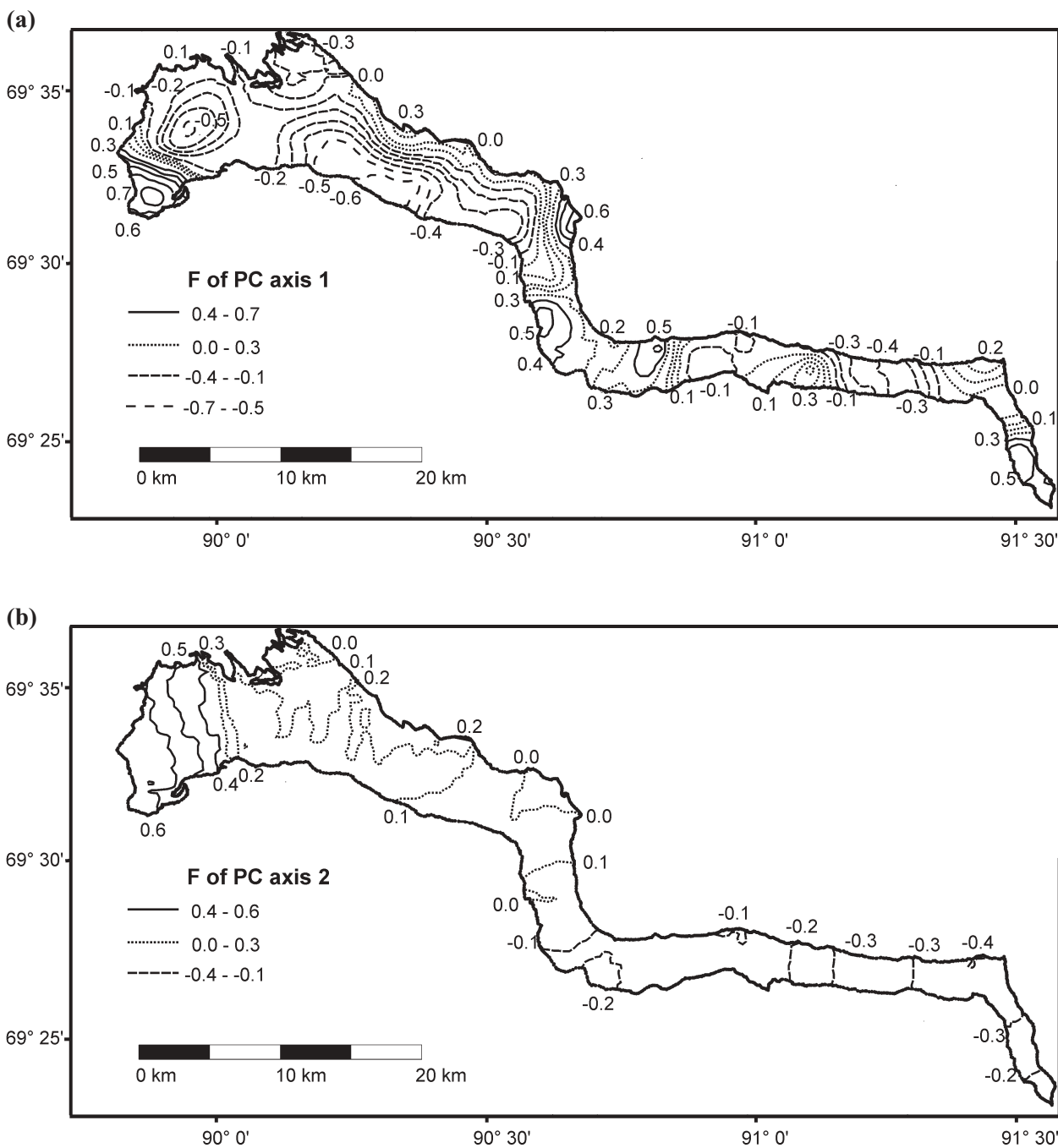


**Figure 4.** Spatial distribution of kriged estimates of the (a) first and (b) second PCs in Lake Lama.

A second prominent feature in the spatial gradients in principal component scores of axis 1 is a region in the middle of the western basin. Here the principal component scores changed from the maximum negative values to positive values up to 0.3 from the southern shore towards the northern shore (Fig. 4a). This variation in principal component scores is caused mainly by a decrease in biogenic silica and partly by an increase in CaO in the northern shore. The decrease in biogenic silica indicates

a change in primary productivity of siliceous algae that is related to diatom assemblage change with decreasing water depth (Kienel and Kumke, 2002).

The most distinct variation in estimates of principal component scores of axis 1 occurred in the shallow water areas of the western end of the western basin. Local minimum and maximum values are separated by only 5 km. Sedimentological properties mainly responsible for these anomalies and the resulting spatial gradients are increas-

ing sand fractions towards the lake outflow and high values of biogenic silica that decrease in the outflow direction. Other sediment components contributing to axis 1 vary little. The increase in biogenic silica is about twofold compared to other values in the region, indicating a higher production of diatoms. Sedimentary diatom assemblages, however, are dominated by periphytic taxa in that part of the lake and the spatial structure of the assemblages (cf. Kienel and Kumke, 2002) is not related to principal component scores. The large sand fractions (up to 83%) and low values of biogenic silica (around one-third of the lake average) near the lake outflow, causing high positive principal component scores, are probably the result of re-suspension and transport of particles by erosion. The shallow water area near the lake outflow is, hence, not a sediment accumulation area. Additionally, this region is subjected to reinforced hydrodynamic processes that affect re-suspension. At the spatial scale of 100s of meters to km, advective currents and wind current patterns are processes influencing the lake ecosystem and, subsequently, the sediments at shallow water depths (Pinel-Alloul, 1995).

The spatial distribution in principal component scores of axis 2 reveals large-scale patterns (Fig. 4b). Values are negative and relatively stable in the eastern tip and the eastern basin of the lake, increase gradually in the north-south link, and become positive in the western basin. Steep spatial gradients only occur in the western part of the western basin where water depth decreases. The spatial structure of the second principal component is related to basin morphology; principal component scores are significantly correlated with water depth ( $r = -0.36$ ,  $P \leq 0.05$ ). Basin morphology is a feature typically influencing lakes at large spatial scales (Pinel-Alloul, 1995; Kienel and Kumke, 2002). The gradual increase in principal component scores is caused by a number of sediment components that slightly, but not significantly, increase from east to west as revealed by ANOVA. Among these components are most of those that contributed to the second principal axis (see Fig. 3). The TOC/TN ratio and Cu showed the opposite trend since they contribute to the opposite direction of the principal axis. However, there are no significant differences between basin averages of the components, apart from  $\delta^{13}\text{C}_{\text{org}}$  and Zr that are significantly lighter or higher at  $P \leq 0.05$ , respectively. In addition, the most distinct differences occurred between the means in TOC/TN ratios of the eastern tip/eastern basin (about 13.5) and the north-south link/western basin (about 11.5). As noted earlier, the largest values in TOC/TN ratio are located near river inlets, pointing to an introduction of material derived from land plants. Differences among basin means could be caused by the higher energy of rivers contributing to Lake Lama in the eastern tip and eastern basin as well as by an increased sediment input by erosion since the morphology of the catchment in the

eastern part is characterized by much steeper slopes than in the western part. Hence, coarse material introduced by rivers could be transported over longer distances by currents and influence a larger area of sediment in the eastern than western part of the lake. In addition, a slumping of coarse material along the steep slopes in the eastern basin could occur and might explain the larger basin mean in sand fraction.

Another prominent feature is the steep spatial gradient in the western part of the western basin. Sedimentary components responsible for these variations are  $\delta^{13}\text{C}_{\text{org}}$ , Zr and partly Nb. Values of Zr and Nb are significantly correlated ( $r = 0.56$ ,  $P \leq 0.05$ ) and increase in the western part of the western basin. Their increase in the sediments of Lake Lama might be related to increased atmospheric deposition since Zr especially is regarded to be a first fall-out from dust due to its inability to be transported over long distances (Sirocko et al., 2000). Increased eolian deposition in the western part of Lake Lama likely occurs because of its vicinity to the city of Norilsk west of Lake Lama (see Fig. 1). Hagedorn et al. (1999) concluded that any anthropogenic deposits, proven to have influenced recent deposits in Lake Lama in their study, can only be transported by wind since there is no discharge of wastewater into the lake. Values of  $\delta^{13}\text{C}_{\text{org}}$  increase in the western part of the western basin, leading to statistically significant differences between the western basin and other parts of Lake Lama. In addition, there was a significant correlation between  $\delta^{13}\text{C}_{\text{org}}$  and water depth ( $r = -0.45$ ,  $P \leq 0.05$ ). The isotopically heavier signatures of organic carbon in the sediments support the assumption that erosional processes are dominating in this part of the lake, leading to exposure of Late Weichselian glaciolacustrine sediments. In this case, sediments were enriched in carbonates from the underlying sedimentary rocks and, consequently, water is harder (Harwart et al., 1999). Assimilation pathways of organisms would have changed from  $\text{CO}_2$  to  $\text{HCO}_3^-$ , leading to an increase of  $\delta^{13}\text{C}_{\text{org}}$  by 9‰ (Meyers and Lallier-Verges, 1999). Additionally, Silurian rocks containing limestone are outcropping directly and uncovered at the western lake border and could increase the hardness of the water. The closest sampling point to the outcrops had the maximum value in  $\delta^{13}\text{C}_{\text{org}}$ . However, since no measurements of pH in the lake are available from this location, these explanations are only probable processes affecting the spatial structure in sediment properties in that part of the lake. The statistical relationship between  $\delta^{13}\text{C}_{\text{org}}$  and water depth indicates that, in general, additional processes might influence the carbon isotope signatures in Lake Lama that cannot be identified by the data.

## Conclusions

Lake Lama is an excellent example showing how physical, chemical and biological lake processes are reflected in lake sediments and how they affect the sediment composition in lakes. The general view that the number of processes at different spatial scales increases with lake size and complexity of the lake system (e.g., Pinel-Alloul, 1995) was observed in the sediments of Lake Lama. Measured sediment properties in this lake are influenced by a variety of processes; e.g., lake morphology and the water depth, the number, size and position of river inflows, catchment morphology and hydrodynamical processes. Each process is characterized by its own spatial scale resulting in a large spatial heterogeneity in sediment properties of Lake Lama. The statistical techniques applied in this study (i.e., principal components analysis and geostatistical analysis) were suitable for extracting and explaining the spatial structure in lake sediments. The use of the first two principal components assured that the major patterns, capturing more than half of the variance, were preserved for geostatistical analysis. Variables that contributed most to the spatial patterns were the particle size, biogenic silica, CaO, TOC/TN ratio,  $\delta^{13}\text{C}_{\text{org}}$  and Zr. Variograms of the first two principal components were quite different in their shape and parameters. The variogram of the first component was characterized by a range of spatial correlation of about 5 km and a relative nugget variance of 34%, whereas the variogram of the second component had a range of approximately 60 km and a relative nugget variance of 21%. Both variograms describe the spatial structure of the respective components and allow one to suggest some processes responsible for that structure. For the first component, we conclude that the dominating processes are related to the material transported and deposited by rivers which strongly affect particle size distributions at river mouths. The second component is largely influenced by lake morphology and the water depth. However, the regionalized, block-kriged maps of the components revealed some more features in sediment spatial structure. For example, the most distinct changes in sediment composition occurred at relatively small spatial scales in the western part of the western basin. These variations are affected by hydrodynamical processes such wind-induced currents and resuspension of material. However, the considerable amount of small-scale variability of both principal components indicates the presence of processes beyond our sampling design.

The results showed the importance of a proper spatial analysis of lake sediments to obtain a representative picture of sediment properties in lakes. The importance is likely to increase with lake size and complexity of the catchment. We, therefore, recommend such analyses prior to conducting paleoenvironmental or paleolimnological studies.

## Acknowledgements

We thank the participants of the expedition Norilsk 97 of the Alfred Wegener Institute for providing us with sample material and field data. We are grateful to T. Boettger for helping us to interpret the carbon isotope distribution. We would like to thank J. Baier, D. Subetto and an anonymous reviewer for helpful comments on earlier drafts of the manuscript.

## References

- Anderson, N. J., 1990. Spatial pattern of recent sediment and diatom accumulation in a small, eutrophic lake. *J. Paleolim.* **3**: 143–160.
- Anderson, N. J., 1998. Variability of diatom-inferred phosphorus profiles in a small lake basin and its implications for histories of lake eutrophication. *J. Paleolim.* **20**: 47–55.
- Andreev, A. A., P. E. Tarasov, V. A. Klimanov, M. Melles, O. M. Lisitsina and H.-W. Hubberten, 2004. Vegetation and climate changes around the Lama Lake, Taymyr Peninsula during the Late Pleistocene and Holocene reconstructed from pollen records. *Quat. Int.* **122**: 69–84.
- Ashley, G. M., 1995. Glaciolacustrine Environments. In: J. Menzies (ed.), *Modern Glacial Environments – Processes, Dynamics and Sediments*. Butterworth-Heinemann Ltd., Oxford, pp. 417–444.
- Ellsworth, T. R. and C. W. Boast, 1996. Spatial structure of solute transport variability in an unsaturated field soil. *Soil Sci. Soc. Am. J.* **60**: 1355–1367.
- Englund, E. and A. Sparks, 1991. GEO-EAS 1.2.1. Geostatistical Environmental Assessment Software – User's guide, US Environmental Protection Agency, Las Vegas.
- Galaziy, G. J. and Y. P. Paramuzin, 1981. Lakes in the North-West of the Siberian Platform (in Russian), Nauka, St. Petersburg.
- Hagedorn, B., S. Harwart, M. M. R. van der Loeff and M. Melles, 1999. Lead-210 dating and heavy metal concentration in recent sediments of Lama Lake (Norilsk Area, Siberia). In: H. Kassens, H. A. Bauch, I. A. Dimitrenko, H. Eicken, H.-W. Hubberten, M. Melles, J. Thiede and L. A. Timokhov (eds.), *Land-Ocean Systems in the Siberian Arctic: Dynamics and History*, Springer Verlag, Berlin, pp. 361–376.
- Håkansson, L. and M. Jansson, 1983. *Principles of Lake Sedimentology*, Springer Verlag, Berlin.
- Harwart, S., 1999. Geochemical weathering trends of a basaltic source rock after the retreat of Late Pleistocene glaciers on the Taymyr Peninsula (Central Siberia) – reconstruction using sedimentary sequences of Lake Lama, PhD thesis, University of Potsdam.
- Isaaks, E. and M. Srivastava, 1989. *An Introduction to Applied Geostatistics*. Oxford University Press, New York.
- Kajak, Z., R. Kacprzak and R. Polkowski, 1965. Tubulat bottom sampler. *Ekol. Polska B* **11**: 159–165.
- Kienel, U. and T. Kumke, 2002. Combining ordination techniques and geostatistics to determine the patterns of diatom distributions at Lake Lama, Central Siberia. *J. Paleolim.* **28**: 181–194.
- Korsman, T., M. B. Nilsson, K. Landgren and I. Renberg, 1999. Spatial variability in surface sediment composition characterised by near-infrared (NIR) reflectance spectroscopy. *J. Paleolim.* **21**: 61–71.
- Kumke, T., 1999. Ion transport through agriculturally used soils of a catchment at the Uelzen Basin – Spatial variability of transport and exchange parameters (in German). *Wissenschaft & Technik Verlag*, Berlin.

- Kumke, T., T. Streck and J. Richter, 1999. Regional pattern of the mobile water fraction in soils as determined by disc infiltrometer experiments. *J. Plant Nutr. Soil Sci.* **162**: 393–400.
- Kumke, T., T. Streck and J. Richter, 2002. Ion transport through unsaturated soils: field experiments and regional simulations. *Eur. J. Soil Sci.* **53**: 57–70.
- Lebo, M. E. and J. E. Reuter, 1995. Spatial variability in sediment composition and evidence for resuspension in a large, deep lake. *Mar. Freshwater Res.* **46**: 321–326.
- Legendre, P. and M.-J. Fortin, 1989. Spatial pattern and ecological analysis. *Vegetatio* **80**: 107–138.
- Legendre, P. and L. Legendre, 1998. *Numerical Ecology*, Elsevier, Amsterdam.
- Lightfoot, P. C., A. J. Naldrett, N. S. Gorbachev, W. Doherty and V. A. Fedorenko, 1990. Geochemistry of the Siberian Trap of the Noril'sk area, USSR, with implications for the relative contributions of crust and mantle to flood basalt magmatism. *Contrib. Mineral. Petr.* **104**: 631–644.
- Meyers, P. A. and R. Ishiwatari, 1995. Organic matter accumulation records in lake sediments. In: A. Lerman, D. M. Imboden and J. R. Gat (eds.), *Physics and Chemistry of Lakes*. Springer Verlag, Berlin, pp. 279–329.
- Meyers, P. A. and E. Lallier-Vergés, 1999. Lacustrine sedimentary organic matter records of Late Quaternary paleoclimates. *J. Paleolim.* **21**: 345–372.
- Naldrett, A. J., P. C. Lightfoot, V. A. Fedorenko, W. Doherty and N. S. Gorbachev, 1992. Geology and geochemistry of intrusions and flood basalts of the Noril'sk region, USSR, with implications for the origin of the Ni-Cu ores. *Econ. Geol.* **87**: 975–1004.
- Pinel-Alloul, B., 1995. Spatial heterogeneity as a multiscale characteristic of zooplankton community. *Hydrobiologia* **301**: 17–42.
- Russo, D., 1984. A geostatistical approach to solute transport in heterogeneous fields and its applications to salinity management. *Water Resour. Res.* **20**: 1260–1270.
- Sirocko, F., D. Garbe-Schönberg and C. Devey, 2000. Processes controlling trace element geochemistry of Arabian Sea sediments during the last 25,000 years. *Global Planet. Chang.* **26**: 217–303.
- Ter Braak, C. J. F. and C. Prentice, 1988. A theory of gradient analysis. *Adv. Ecol. Res.* **18**: 271–317.
- Webster, R., 1985. Quantitative spatial analysis of soil in the field. *Adv. Soil Sci.* **3**: 1–70.
- Webster, R. and M. A. Oliver, 2000. *Geostatistics for Environmental Scientists*, Wiley, Chichester.
- Yates, S. R. and M. V. Yates, 1990. *Geostatistics for waste management: User's Manual for the GEOPACK (Version 1.0) Geostatistical Software System*, US Environmental Protection Agency, Ada.



To access this journal online:  
<http://www.birkhauser.ch>

---